

# Controlled Synthesis of Water-Dispersible Faceted Crystalline Copper Nanoparticles and Their Catalytic Properties

Yanfei Wang,<sup>[a, b]</sup> Ankush V. Biradar,<sup>[a, b]</sup> Gang Wang,<sup>[c]</sup> Krishna K. Sharma,<sup>[c]</sup>  
Cole T. Duncan,<sup>[c]</sup> Sylvie Rangan,<sup>[d]</sup> and Tewodros Asefa\*<sup>[a, b]</sup>

**Abstract:** We report a solution-phase synthetic route to copper nanoparticles with controllable size and shape. The synthesis of the nanoparticles is achieved by the reduction of copper(II) salt in aqueous solution with hydrazine under air atmosphere in the presence of poly(acrylic acid) (PAA) as capping agent. The results suggest that the pH plays a key role for the formation of pure copper nanoparticles, whereas the concentration of PAA is important for controlling the size and geometric shape of the nanoparticles. The average size of the copper nanoparticles can be

varied from 30 to 80 nm, depending on the concentration of PAA. With a moderate amount of PAA, faceted crystalline copper nanoparticles are obtained. The as-synthesized copper nanoparticles appear red in color and are stable for weeks, as confirmed by UV/Vis and X-ray photoemission (XPS) spectroscopy. The faceted crystalline copper nanoparticles serve as an effective cata-

lyst for N-arylation of heterocycles, such as the C–N coupling reaction between *p*-nitrobenzyl chloride and morpholine producing 4-(4-nitrophenyl)morpholine in an excellent yield under mild reaction conditions. Furthermore, the nanoparticles are proven to be versatile as they also effectively catalyze the three-component, one-pot Mannich reaction between *p*-substituted benzaldehyde, aniline, and acetophenone affording a 100% conversion of the limiting reactant (aniline).

**Keywords:** heterogeneous catalysis • copper • nanoparticles • poly(acrylic acid) • shape control • size control

## Introduction

Noble metal nanoparticles have attracted considerable attention owing to their potential applications in fields such as catalysis, biology, electronics, and information technology.<sup>[1–4]</sup>

Copper nanostructures are expected to be essential components in future nanodevices and nanocircuits due to their excellent electrical conductivity.<sup>[5–7]</sup> Copper nanoparticles are also widely used as catalysts for various reactions including water–gas shift<sup>[8]</sup> and gas detoxification reactions,<sup>[9]</sup> and as electrocatalysts in solid oxide fuel cells.<sup>[10]</sup> On the other hand, due to their good biocompatibility and surface-enhanced Raman scattering (SERS) properties, copper nanoparticles may have potential applications as nanoprobes in medical diagnosis and biological analysis.<sup>[2b]</sup> Like many other nanomaterials, the size and shape of copper nanoparticles have a significant effect on their electronic, catalytic, and optical properties. Therefore, the preparation of monodispersed copper nanoparticles with controlled size and shape along with the investigation of their catalytic properties remains to be of considerable interest.

A number of different methods have been reported for the preparation of copper nanostructures. The first approach is a surfactant-assisted reduction method involving the chemical reduction of copper ions in an aqueous solution in the presence of various capping agents.<sup>[11–19]</sup> For instance, mixed reverse micelles as a template have been used to synthesize and control the size and shape of copper nanoparti-

[a] Dr. Y. Wang, Dr. A. V. Biradar, Prof. T. Asefa  
Department of Chemistry and Chemical Biology, Rutgers  
The State University of New Jersey, 610 Taylor Road  
Piscataway, NJ 08854 (USA)  
Fax: (+1) 732-445-5312  
E-mail: tasefa@rci.rutgers.edu

[b] Dr. Y. Wang, Dr. A. V. Biradar, Prof. T. Asefa  
Department of Chemical Engineering and Biochemical Engineering  
Rutgers, The State University of New Jersey  
98 Brett Road, Piscataway, NJ 08854 (USA)

[c] G. Wang, Dr. K. K. Sharma, C. T. Duncan  
Department of Chemistry, Syracuse University, 111 College Place  
Syracuse, NY 13244 (USA)

[d] Dr. S. Rangan  
Department of Physics and Astronomy, Rutgers  
The State University of New Jersey  
136 Frelinghuysen Rd, Piscataway, NJ 08854 (USA)

Supporting information for this article is available on the WWW under <http://dx.doi.org/10.1002/chem.201000354>.

cles.<sup>[11]</sup> Furthermore, by using sodium dioctyl sulfosuccinate (AOT)–water–oil reverse micellar systems, copper nanoparticles, nanorods, and nanodisks, the sizes and shapes of which were controlled by regulating the water content in the oil phase and/or the concentration of reducing agent or salt, were synthesized.<sup>[12–15]</sup> Other capping agents such as cetyltrimethylammonium bromide (CTAB),<sup>[16]</sup> sodium dodecylbenzene sulfonate (DBS),<sup>[17]</sup> ethylenediamine (EDA),<sup>[18]</sup> and poly(vinylpyrrolidone) (PVP)<sup>[19]</sup> were also successfully used to synthesize copper nanoparticles with shapes including spheres, cubes, and wires, from the reduction of Cu(OH)<sub>2</sub> with hydrazine in the presence of these surfactants. The second synthetic approach to generate copper nanoparticles is performed in high-boiling-point organic solvents by decomposing various types of copper complexes at an elevated reaction temperature in the presence of capping agents. For instance, copper nanoparticles with different shapes such as rods and cubes were synthesized by decomposing [Cu(acac)<sub>2</sub>] (acac=acetylacetonate) in octyl ether with oleic acid or oleyl amine capping agent at different reaction temperatures.<sup>[20]</sup> The formation of the shaped nanoparticles was attributed to three sequential events: initial nucleation of seed metal clusters, preferential adsorption of capping agents on selected facets of the seed nanocrystal, and anisotropic growth of the metal in the other facets. Similarly, shaped Cu nanoplates with intense plasmon resonances were also obtained in *N,N*-dimethylformamide (DMF) solvent.<sup>[21]</sup> In the third synthetic approach, called the polyol reduction method, ethylene glycol serves as the solvent and the reductant for copper ions with PVP capping agent to produce copper nanomaterials.<sup>[22]</sup> The fourth reported method involves bioinspired synthetic routes that use a histidine-containing peptide backbone to synthesize and control the size of copper nanomaterials.<sup>[23]</sup> The conformational changes in the peptide backbone have been correlated to the size and the degree of dispersity of the nanoparticles.<sup>[23]</sup> Finally, physical vapor deposition,<sup>[24,25]</sup> chemical vapor deposition,<sup>[26]</sup>  $\gamma$  irradiation,<sup>[27]</sup> irradiation with UV light,<sup>[28]</sup> and sonochemical methods<sup>[29]</sup> have been reported for the synthesis of copper nanostructures. However, the development of aqueous-phase synthetic methods to shaped copper nanoparticles has been rarely explored because the propensity of surface oxidation of copper makes it difficult to fabricate chemically stable Cu colloids.

Herein, we report an aqueous-phase synthetic route to pure faceted crystalline copper nanoparticles with tunable size and shape. The synthesis involves the reduction of copper(II) salts with hydrazine in presence of poly(acrylic acid) (PAA) capping agent. By adding different amounts of PAA, copper nanoparticles with tunable sizes and shapes were obtained. For instance, the average size of the copper nanoparticles was varied between 30 to 80 nm by simply changing the concentration of PAA. Furthermore, the pH of the solution was determined to play a key role for the formation of pure copper nanoparticles as opposed to copper oxide nanoparticles. By adjusting the amount of PAA, faceted crystalline copper nanoparticles were obtained. These as-prepared

faceted crystalline copper nanoparticles showed high catalytic activity towards N-arylation of heterocycles by C–N coupling between aryl halides and N-heterocycles under mild and aerated reaction conditions. Furthermore, the Cu nanoparticles effectively catalyzed the Mannich coupling reaction of three reactants (*para*-substituted benzaldehyde, aniline, and acetophenone) in one pot.

## Results and Discussion

**Synthesis of copper nanoparticles by optimizing the pH of the solution (effect of pH):** Although the chemistry and most of the procedures we used to make copper nanoparticles and the ones previously reported for making copper(I) oxide nanowires<sup>[30]</sup> are similar, the two syntheses resulted in completely different types of nanomaterials. In the synthesis of copper(I) oxide nanowires, the primary reaction involves the reduction of copper(II) salts with hydrazine in PVP producing yellowish-colored samples of Cu<sub>2</sub>O nanowires. Here in our case, the key modification of using PAA as capping agent resulted in faceted crystalline copper nanoparticles instead of copper(I) oxide, although the same reduction step was employed. In aqueous solution, the chains of the PAA polymer extend from the copper nanoparticle surface and provide the nanoparticles steric stabilization from aggregation. It is also worth mentioning that the synthetic route with PVP capping agent<sup>[30]</sup> does not produce pure copper nanoparticles even in a wide pH range. Although our synthetic method is somewhat similar to the one described in reference [30], the use of PAA as a capping agent made the pH optimum enough to favor the formation of pure copper rather than copper oxide. An additional advantage of the PAA capping agent is the extension of its uncoordinated carboxylate groups into aqueous solution conferring the particles a high degree of dispersion in water.

Figure 1 shows typical UV/Vis absorption spectra of PAA-capped copper nanoparticles that were synthesized at various pH values and a graph of their absorption maxima versus the pH. The UV/Vis absorption spectra of the as-prepared copper nanoparticles display a well-defined absorption peak at around  $\lambda = 565$  nm (Figure 1A). The absorption peak can be attributed to the excitation of plasmon resonance or interband transition, which is a characteristic property of the metallic nature of copper nanoparticles.<sup>[31]</sup> The appearance of this absorption peak further indicates the reduction of copper ions into copper nanoparticles under our synthetic conditions.

Our studies indicated that setting the pH of the solution to an appropriate value played an important role to obtain pure copper nanomaterial as opposed to copper oxide nanomaterial. Copper nanoparticles are only formed if the final pH of the solution ranges between 9.2–10.5. From the UV/Vis absorption spectra obtained at various pH values (Figure 1), it was obvious that the intensity and position of the absorption maxima changed at different pH values. At lower pH (i.e., 9.2–10.3), the spectra exhibited an absorb-

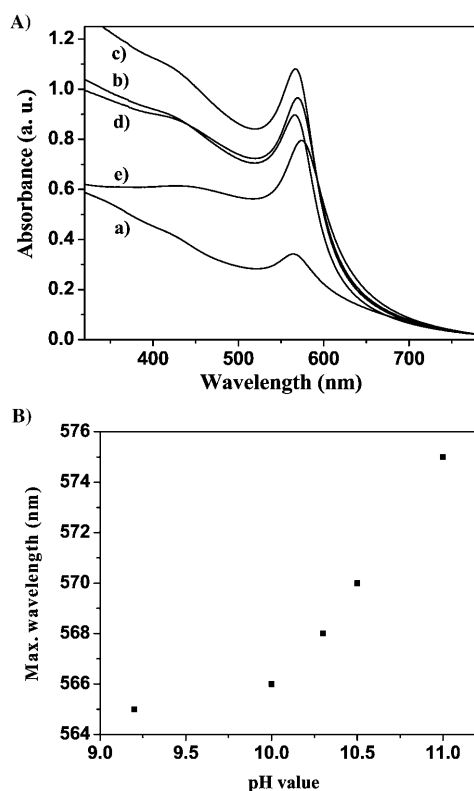


Figure 1. A) UV/Vis absorption spectra of copper nanoparticles synthesized in 1.0 mM aqueous PAA solution at different pH: a) 9.2, b) 10.0, c) 10.3, d) 10.5, and e) 11.0. B) Absorption maximum of copper nanoparticles versus the pH value.

ance maximum at  $\approx 565$  nm, the characteristic plasmon absorption band for copper nanoparticles. The intensity of this plasmon peak markedly increased when the pH increased from 9.2 to 10.3, indicating the increase in the number or yield of copper nanoparticles. At a slightly higher basicity (or at pH 10.5), the absorption maximum appeared at  $\lambda = 570$  nm. When the pH of the solution was increased to 11.0 with the addition of more NaOH, the UV/Vis absorption peak shifted to 575 nm, whereas its absorption intensity decreased. It has been reported that metallic copper nanoparticles that are surrounded by a copper oxide shell are characterized by a peak centered at about  $\lambda = 570$  nm with a residual absorption peak at  $\lambda = 800$  nm.<sup>[32]</sup> Thus, the absorption maximum at 575 nm that we have observed for the sample synthesized at pH 11.0 could be attributed to the formation of copper nanoparticles with a copper oxide monolayer around them.<sup>[32]</sup> However, it is worth noting that the absorption maximum at 800 nm was not observed in the latter case, implying that the copper oxide shell is only a thin monolayer, if any. This was further confirmed by X-ray photoelectron spectroscopy (XPS; see below). It can be concluded that in the pH range of 10.5–12.0, a very low proportion of copper atoms on the copper nanoparticles form copper oxide. However, upon raising the pH to 12.0 by adding more NaOH, we observed the exclusive formation of  $\text{Cu}_2\text{O}$  nanoparticles. The obtained trend in the absorption

maxima of the copper nanoparticles with respect to the pH values is also consistent with that reported in reference [33] for copper oxide and alkanethiol-capped copper nanoparticles synthesized in supercritical water, except for a minor difference. In the case described in reference [33], pH < 6.0 favored the formation of copper nanoparticles and pH > 6.0 resulted in oxidized products from the reactions of copper ions with excess hydroxyl groups.<sup>[33]</sup> Whereas we have also observed the formation of a mixture of polymer-capped copper/copper oxide nanoparticles or pure copper oxide nanoparticles from  $\text{CuSO}_4$  in the presence of PAA, this was observed at significantly higher pH; that is, copper oxide nanoparticles at pH  $> \approx 10.5$  and metallic copper nanoparticles between pH 9.2–10.5. It should be emphasized again that the pH range that produces copper versus copper oxide varies for different surface ligands; that is, whether alkanethiol, PAA, or PVP are used as capping agent during the synthesis of the nanoparticles. The latter observation can be explained on the basis of the  $\text{p}K_a$  values of these capping agents. PAA has a  $\text{p}K_a$  value of 4.0. In the range of pH  $\approx 9.5$ –10.5, where we obtained copper nanoparticles, PAA exists predominantly in its negatively charged form because of significant abstraction of its acidic protons by the basic solution. Besides serving the purpose of reducing the hydroxyl ion concentration in the solution, the negatively charged PAA polymer will cap the copper nanoparticles better. However, as the ligands such as PVP and alkanethiol do not react with or reduce the hydroxyl ions, all the hydroxyl groups will react with the copper ions to form copper oxides, even at relatively lower starting pH. Our studies demonstrated that the reduction of copper(II) ions with hydrazine in the presence of PAA capping ligand in an appropriate pH range of 9.2–10.5 yields polymer-coated and water-dispersible pure copper nanoparticles, whose yield is dependent on the pH of the solution as shown in Figure 1 A. The as-synthesized copper nanoparticles appear red in color and are stable for weeks as also observed by UV/Vis spectroscopy. These nanoparticles were quite stable as their plasmon band barely changed even after eight weeks (see the Supporting Information, Figure S1).

XPS is widely used to confirm the chemical composition of copper nanoparticles.<sup>[7]</sup> In particular, the peak corresponding to the  $\text{Cu}(2p_{3/2})$  core level is commonly used to analyze the degree of oxidation of Cu. Figure 2 shows the XPS spectra of the copper nanoparticles synthesized with the method presented here. The reference peak for C1s was set at 284.7 eV. The major peak for  $\text{Cu}(2p_{3/2})$  was observed at 932.8 and 932.5 eV for the samples prepared with 1.0 and 2.0 mM PAA, respectively. This peak can be attributed to zerovalent copper.<sup>[7a,e-n]</sup> Furthermore, a peak for  $\text{Cu}(2p_{1/2})$  was observed at 952.7 and 952.3 eV, respectively, which also correspond to  $\text{Cu}^0$ . Peaks corresponding to  $\text{Cu}^{2+}$  were barely observed, ruling out the possibility of the presence of  $\text{CuO}$  or  $\text{Cu}(\text{OH})_2$  in these samples. However, as shown in Table 1 and as reported by others,<sup>[7]</sup> the  $\text{Cu}(2p_{3/2})$  peaks for  $\text{Cu}^+$  and  $\text{Cu}^0$  overlap. Consequently, our result can not rule out the presence of  $\text{Cu}_2\text{O}$ . In fact, a small oxygen peak was

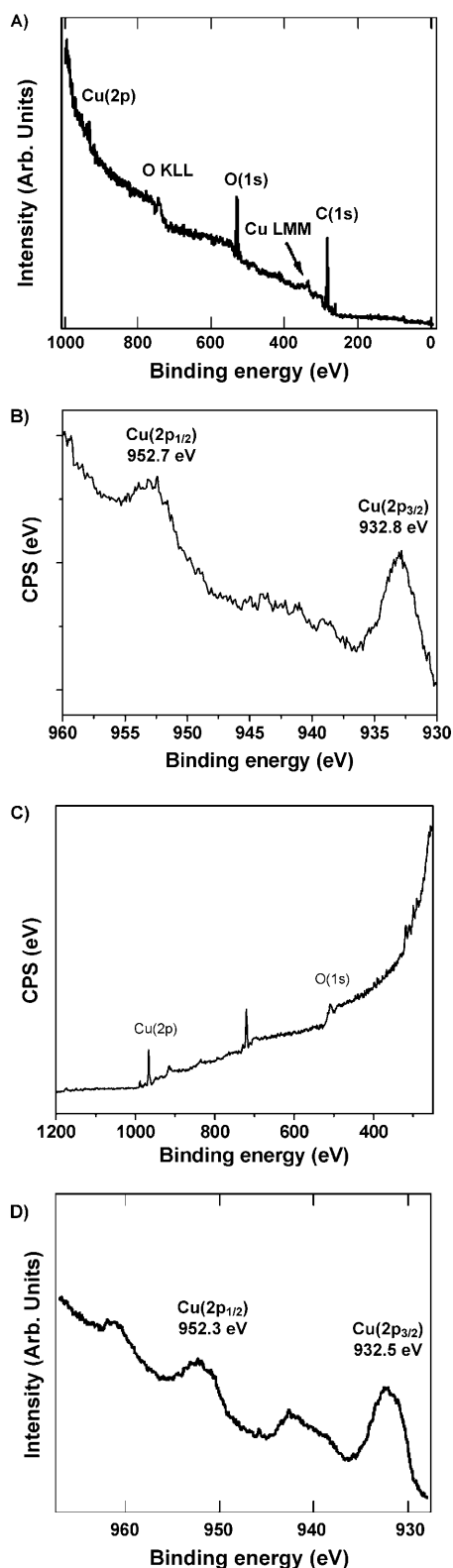


Figure 2. A,B) X-ray photoelectron spectra of copper nanoparticles prepared with 1.0 mM PAA showing: A) all the main peaks and B) the peaks corresponding to Cu(2p<sub>3/2</sub>) and Cu(2p<sub>1/2</sub>). C,D) X-ray photoelectron spectra of copper nanoparticles prepared with 2.0 mM PAA showing: C) all the main peaks and D) the Cu(2p<sub>3/2</sub>) and Cu(2p<sub>1/2</sub>) peaks.

Table 1. XPS data for Cu and for its oxidized forms.

Materials/compound	Binding energy [eV]		Reference
	Cu(2p <sub>3/2</sub> )	Cu(2p <sub>1/2</sub> )	
Cu <sup>0</sup>	932.7–932.8		[7e]
	932.6		[7f,g–i]
	932.9	952.7	[7m]
Cu <sub>2</sub> O	932.5–932.8		[7e]
	932.6		[7h–i]
CuO	933.5–933.6		[7e]
	933.8		[7f,h,j]
Cu(OH) <sub>2</sub>	934.0		[7i]
	934.6		[7f]
	934.7		[7k]
	935.0		[7g,i,l]

also observed as described in references [7m] and [7n]. Based on previous results (ref. [7]), we have assigned the small oxygen peak to be due to the presence of a small Cu<sub>2</sub>O layer around the nanoparticles. Nevertheless, we wish to emphasize that this oxide layer is a result of the unavoidable exposure of the samples to air and the necessity of being in a dried form for the XPS measurement. In fact, we noticed a slight color change of the sample to greenish color during this measurement. Their reddish color and their UV/Vis absorption maxima remained unchanged when they were in solution suggesting that they were purely metallic copper nanoparticles in solution. Upon deliberate exposure of the dried copper nanoparticle samples to air for longer time, a significant portion of the nanoparticles was oxidized to CuO or Cu(OH)<sub>2</sub><sup>[7]</sup> (Figure S1 in the Supporting Information). Figure S2 in the Supporting Information shows a major peak at 933.1 eV and some satellite peaks at 943.1 and 939.9 eV, which correspond to Cu(2p<sub>3/2</sub>) of CuO,<sup>[7]</sup> for copper nanoparticles left under air for a week.

**Controlling the size and shape of PAA-capped copper nanoparticles:** Controlling the nanoparticle size and shape can provide an elegant strategy for tuning optical properties of nanomaterials. Here, the size and shape of the copper nanoparticles were found to strongly depend on the concentration of PAA. The size of the nanoparticles can be decreased from ≈80 to ≈30 nm simply by increasing the amount of PAA while keeping all other parameters, including the pH, fixed. Figure 3 shows the TEM images of the nanoparticles obtained by using a higher amount of PAA protecting agent. The TEM images further confirm the formation of nanoscale copper material with varying diameter and interesting morphologies. When the concentration of PAA was low (1.0 mM), the nanoparticles were large and most of them had spherical shape. The average diameter for these copper nanoparticles was ≈80 nm. When the PAA concentration was increased to 1.33 mM, faceted crystalline Cu nanoparticles with edge length of approximately 50 nm were formed (Figure 3B). At a PAA concentration of about 2.0 mM, the size of the nanoparticles decreased whereas their polydispersity increased. The TEM images showed that the size of the nanoparticles decreased from 80 to 30 nm

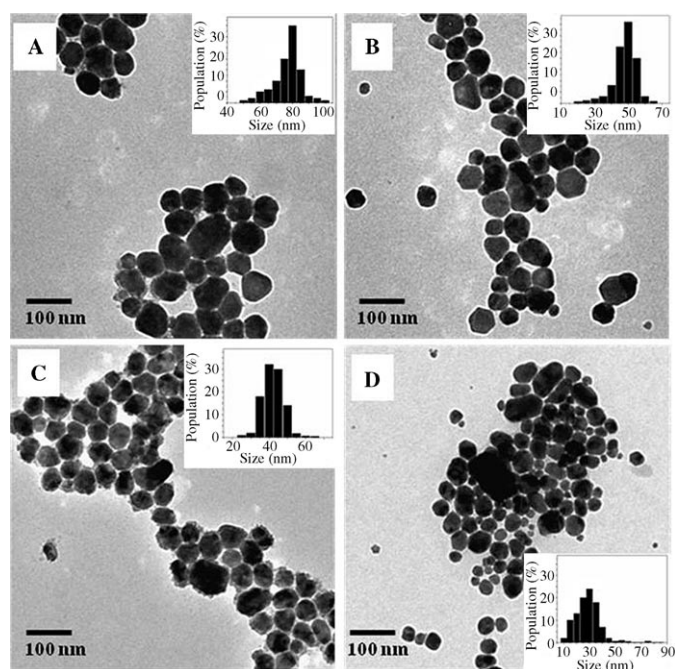


Figure 3. TEM images of copper nanoparticles synthesized in aqueous PAA solution with different concentration: A) 1.0, B) 1.33, C) 1.66, and D) 2.0 mM.

upon increasing the PAA concentration from 1.0 to 2.0 mM. This is consistent with the fact that the protecting effect of the polymer increases with its concentration favoring the formation of smaller nanoparticles.

In addition to tuning the sizes of nanoparticles, a certain amount of PAA was also indispensable in controlling the morphology of the copper nanoparticles. The TEM images (Figure 3) showed that most of the nanoparticles synthesized with lower PAA concentration (1.0 mM) had spherical shape. The increase of the PAA concentration from 1.0 to 1.66 mM and 2.0 mM induced the formation of some smaller spherical copper nanoparticles as well as some elongated nanoparticles (or nanorods) with an aspect ratio of  $\approx 2$  (Figure 3).

Interestingly, with a moderate amount of PAA (1.33 mM), nanoparticles with predominantly faceted crystalline structure that look more like cuboctahedral-shaped were formed (Figure 3B). Hence, varying the PAA concentration not only induces a change in the size of the copper nanoparticles, but also tunes their shapes. An enlarged TEM image for the sample prepared by adjusting the PAA concentration to 1.33 mM is shown in Figure 4A. It reveals many well-truncated cuboctahedron-shaped copper nanoparticles. These cuboctahedral-shaped nanoparticles exhibit a projection of hexagonal shape with an average edge length of 50 nm. It is well known that a cuboctahedral particle lying on a flat surface against one of its faces rather than its corner or edge also shows a projection of hexagon. But the octahedral nanoparticles usually exhibit two differently projected shapes, namely, a rhombus and a hexagon, depending on their orientation relative to the electron beam. Here, the

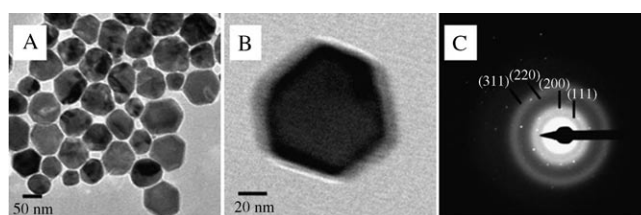


Figure 4. A) TEM images of faceted crystalline copper nanocrystals prepared by using a 1.33 mM PAA solution. B) TEM image of an individual faceted crystalline copper nanoparticle. C) Electron diffraction (ED) pattern of an individual faceted crystalline nanoparticle.

rhombus shape was not observed, which excluded the possibility of the octahedral shape. So the as-synthesized copper nanoparticles must have cuboctahedral shape. Figure 4B shows a representative TEM image of the hexagon, consistent with the hexagonal projection of an ideal cuboctahedron. Typical TEM images of a copper nanoparticle before and after tilting by  $30^\circ$  are shown in Figure S3 in the Supporting Information. The TEM images show that the shape of the particle did not change when the particle was tilted by  $30^\circ$ , indicating that the copper nanoparticles were cuboctahedral in shape. It is worth mentioning that in this cuboctahedron projection, four  $\{111\}$  and two  $\{100\}$  facets are placed on the edges of the hexagonal shape. Other facets represent the projections from the cuboctahedral structure along different orientations. The corresponding selected-area electron diffraction (SAED) patterns of the nanoparticles are shown in Figure 4C. The SAED patterns showed diffraction rings corresponding to 111, 200, 220, and 311 characteristic reflections. Unfortunately, our attempts to get scanning electron microscopy (SEM) images for the particles did not yield clear images because of the continuous change of the shapes and morphologies of the copper nanoparticles in the electron beam, possibly due to melting, as well as oxidation of the surface of the nanoparticles into a non-conducting copper oxide. In fact, the nanoparticles continuously get fuzzier while under the beam for longer and longer time during imaging. Coating the particle's surface with carbon and lowering the electron beam did not help either. Nonetheless, some SEM images were obtained and these are shown in Figure S4 in Supporting Information. These SEM images still exhibit particles with shaped morphologies, although the shapes are not quite clear.

The size-controlled copper nanoparticles that were described in Figure 3 were further characterized by UV/Vis absorption spectroscopy. Figure 5 shows the UV/Vis absorption spectra and digital images of the aqueous dispersions of copper nanoparticles, which were synthesized by using different concentrations of PAA. As observed from the absorption spectra, the absorption bands of the copper nanoparticles strongly depend on the concentration of PAA. At higher PAA concentration (1.66 and 2.0 mM), the absorption spectra of the copper nanoparticles showed plasmon peaks centered at 562 and 560 nm, respectively. For the faceted crystalline copper nanoparticles, which corresponds to a

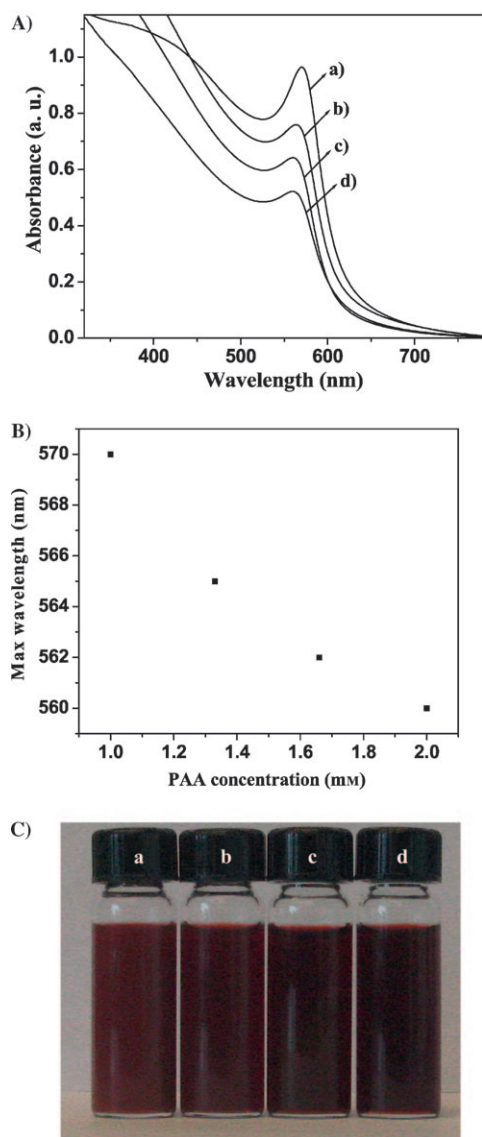


Figure 5. A) UV/Vis absorption spectra of copper nanoparticles synthesized in aqueous PAA solution of different concentration: a) 1.0, b) 1.33 mM, c) 1.66, and d) 2.0 mM. B) Absorption maximum of the copper nanoparticles versus the PAA concentration. C) Photograph of solutions of copper nanoparticles synthesized with different PAA concentration: a) 1.0, b) 1.33, c) 1.66, and d) 2.0 mM.

PAA concentration of 1.33 mM, the absorption spectrum is characterized by a maximum centered at 565 nm. At low PAA concentration (1.0 mM), the absorption maximum is centered at 570 nm. It is interesting to note that the optical absorption of the copper nanoparticles synthesized from PAA concentration of 1.0 mM exhibited another shoulder around 430 nm. With an increase in the PAA concentration from 1.0 to 2.0 mM, we clearly observed a shift of the absorption maxima of  $\approx 10$  nm (Figure 5B). It has been reported that a peak centered at 560 nm can be attributed to spherical and cuboctahedral copper nanocrystals.<sup>[34]</sup> On the other hand, a resonance in the absorption spectrum at lower energies was reported for copper nanocrystals having a

marked change in shape.<sup>[35]</sup> Therefore, based on this previous reports, the shift of the absorption maxima may also be attributed to the different shapes of the copper nanoparticles. Furthermore, shifts in absorption maxima are often attributed to changes in the size of nanoparticles. For example, in the case of Ag nanoparticles, a redshift of 14 nm was reported as the particle size change,<sup>[36]</sup> which is consistent with the general trend that the plasmon maximum shifts to longer wavelength with an increase in particle size.<sup>[37]</sup> Hence, the redshifts that we observed for the absorption maxima of the copper nanoparticles in Figure 5B could be attributed to the changes in size and/or shape of the nanoparticles. However, as both the sizes and shapes of the Cu nanoparticles changed, it is not clear what may have contributed most to this shift of the absorption maxima.

The sizes of the nanoparticles were further analyzed by dynamic light scattering (DLS) (Figure S5 and S6 in the Supporting Information). Two samples of the copper nanoparticle that were prepared with PAA concentration of 1.33 and 2.0 mM were investigated. The results showed that the nanoparticles prepared with a 1.33 mM solution of PAA have an average particle size of 85.5 nm (Figure S2 in the Supporting Information), whereas the nanoparticles prepared with a 2.0 mM solution of PAA exhibited an average particle size of 118.4 nm (Figure S3 in the Supporting Information). These sizes were expectedly higher than those obtained by TEM for the corresponding samples. This is because DLS measurements take the hydrodynamic radius of the polymer around the nanoparticles into account.

Figure 5C displays digital images of aqueous solutions of PAA-capped copper nanoparticles, which show colors ranging from reddish-brown to deep wine-red, depending on the PAA concentration used in the synthesis. It is also worth noting that the greenish color associated with copper(I) and copper(II) oxide nanoparticles was absent, further indicating that the solutions possessed most likely pure copper nanoparticles.

Figure 6 displays the powder X-ray diffraction (XRD) pattern of the as-synthesized copper nanoparticles. The diffraction peaks at  $2\theta = 43.5, 50.6,$  and  $74.3^\circ$  can be indexed as

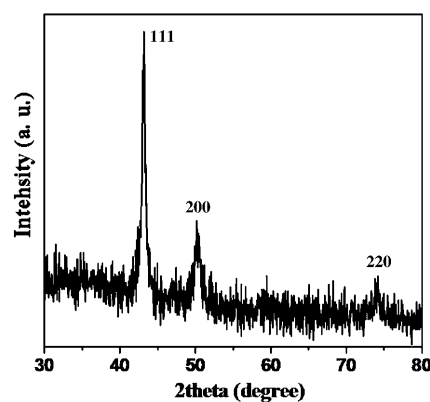
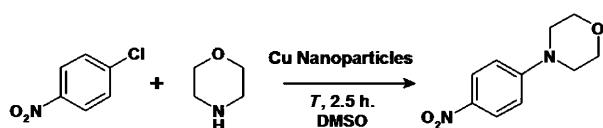


Figure 6. XRD pattern of copper nanoparticles synthesized with a 1.0 mM PAA solution.

the [111], [200], and [220] planes of copper nanoparticles. These results are also quite consistent with those reported previously for metallic copper.<sup>[38]</sup> Furthermore, no diffraction peaks corresponding to copper oxides were detected, confirming the purity of the copper nanoparticles obtained by this synthetic method. This result is also consistent with the XPS data.

**Catalytic activity:** Metal-catalyzed C–N coupling reactions of aryl halides and heterocycles is an important reaction<sup>[39]</sup> as its products have a wide range of applications in medicinal,<sup>[40]</sup> biological,<sup>[41]</sup> and N-heterocyclic carbene chemistry.<sup>[42]</sup> Copper, as well as Cu/Cu<sub>2</sub>O/CuO nanostructures, are reported to be highly active catalysts for C–N coupling and oxidation reactions.<sup>[7c,43]</sup> On the other hand, metal nanocrystals with large number of edge and corner atoms are known to have improved catalytic performance.<sup>[44]</sup> Furthermore, the reactivity and selectivity of a nanocatalyst can depend on its shape, which influences the number and type of atoms located at the edges or corners.<sup>[45]</sup> Therefore, we have evaluated the catalytic performance of the faceted crystalline copper nanoparticles that we have synthesized for N-arylation of heterocycles (Scheme 1).<sup>[46]</sup>

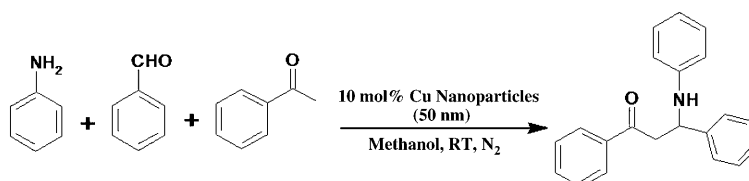


Scheme 1. Nanoparticles-catalyzed C–N coupling reaction.

The materials gave a complete conversion of the starting material in 2.5 h reaction time with a selectivity of  $\approx 99\%$  for the N-arylation product. The product was confirmed by <sup>1</sup>H NMR and FTIR spectroscopy (see the Experimental Section and Figures S9 and S10 in the Supporting Information). These results prove that the cuboctahedron-shaped copper nanoparticles might be used as catalysts for a very valuable and difficult to do C–N coupling reaction. The N-arylation of heterocycles is often performed in the presence of a base such as cesium carbonate.<sup>[46]</sup> In the presence of a high concentration of cesium carbonate at 120 °C, the copper nanoparticles could undergo some oxidation and a color change from reddish to greenish is observed (Figure S7 and S8 in the Supporting Information). The resulting oxidized copper nanoparticles also show catalytic activity. The latter is not surprising as many earlier reports have suggested that both copper and copper oxide and even their combinations as Cu/Cu<sub>2</sub>O/CuO serve as active catalysts for various types of C–C coupling reactions.<sup>[7c,43c,47]</sup>

These Cu nanoparticles were proven to be versatile in their catalytic activities. As previously reported in the litera-

ture, we have conducted the three component Mannish reaction (Scheme 2) by using our Cu nanoparticles as a catalyst. In the presence of a slight amount of base (CsCO<sub>3</sub>), 53 % yield of the three-component Mannish product were ob-



Scheme 2. Nanoparticles-catalyzed Mannich reaction between acetophenone, benzaldehyde, and aniline.

tained in 24 h at room temperature; remaining reactants ended up by forming the imine byproduct. After the reaction, the nanoparticles were found to remain stable and did not aggregate. As shown in the TEM images in Figure S11 in the Supporting Information, the sizes of the nanoparticles were unchanged after catalysis, but the edges of the faceted crystalline structure were slightly destroyed. Furthermore, the UV/Vis spectra of the nanoparticles after the reaction showed a change in the position of the absorption maxima, indicating some oxidation after catalysis. The catalytic performance of the nanoparticles was also lower, giving 3 times less reactant conversion in the same period of reaction time compared to the original sample.

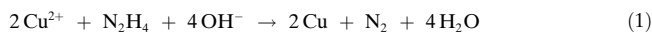
## Conclusion

In summary, we have successfully demonstrated the synthesis of water-dispersible, cuboctahedron-shaped pure copper nanoparticles by reducing Cu<sup>2+</sup> with hydrazine at an appropriate pH in the presence of PAA as protecting agent. The shape and diameter of the nanoparticles were tuned by varying the concentration of PAA in the solution. We have demonstrated that cuboctahedral-shaped copper nanoparticles can be obtained by using moderate concentration of PAA. With increase in the size of the copper nanoparticles, a red-shift in the UV/Vis absorption band was observed. The as-synthesized cuboctahedral copper nanoparticles showed high catalytic activity in promoting C–N coupling reactions, as demonstrated by the reaction between *p*-nitrobenzyl chloride and morpholine forming 4-(4-nitrophenyl)morpholine in an excellent yield and good selectivity (Figure S9 and S10 in the Supporting Information). Furthermore, the nanoparticles were proven to catalyze the three-component, one-pot Mannich reaction giving selectively the Mannich product. In addition, to stabilize the nanoparticles and offer them water dispersibility, the carboxylic acids of the PAA capping ligand can potentially be used as an abundant anchoring point for further attachment of other functional groups and bioactive species for bioanalysis by using the surface enhanced Raman scattering (SERS) property of copper nanoparticles.

## Experimental Section

**Materials and reagents:** Copper(II) sulfate, hydrazine hydrate solution ( $\text{N}_2\text{H}_4\cdot\text{H}_2\text{O}$  solution; 78–82%), poly(acrylic acid) (PAA;  $M_w=1,800$ ), *p*-nitrobenzyl chloride, morpholine, aniline, benzaldehyde, acetophenone, and cesium carbonate were obtained from Sigma–Aldrich. Sodium hydroxide (98.8%) and dimethyl sulfoxide (DMSO) were purchased from Fisher Scientific. All the chemicals were directly used as received without further treatment.

**Synthesis of copper nanoparticles:** In a typical synthesis of copper nanoparticles, a mixture of  $\text{CuSO}_4$  (0.10 mmol) and various amount of PAA were completely dissolved in nanopure  $\text{H}_2\text{O}$  (20 mL) under vigorous stirring at 60°C for 20 min, giving a transparent light-blue solution. The PAA concentration varied from 1.0–2.0 mM. Then, 0.95–1.2 mL NaOH (0.5M) was added dropwise to the solution to adjust the pH. Precipitation of copper(II) hydroxide or copper oxides was not observed because the pH was not high enough. After the solution was stirred for 20 min at 60°C, a solution of  $\text{N}_2\text{H}_4\cdot\text{H}_2\text{O}$  (2.0 mmol) was added to the solution with constant stirring. The reaction flask was kept in a water bath at 60°C for 30 min, and the particles were allowed to age for 24 h at room temperature. It should be pointed out that both NaOH and  $\text{N}_2\text{H}_4\cdot\text{H}_2\text{O}$  can affect the pH of the final solution. The metallic copper nanoparticles in this work were produced following the redox reaction given in Equation (1) under basic conditions.



**Characterization:** Samples for transmission electron microscopy (TEM) were prepared by casting a drop of the as-prepared copper nanoparticles suspension on a carbon-formvar-coated copper grid. The grid was then placed under a JEOL 1200 EX and FEI Tecnai T12 TEM transmission electron microscopes. The images were taken at an acceleration voltage of 120 kV. The UV/Vis absorbance spectra were measured with a Lambda 950 spectrophotometer (PerkinElmer). The X-ray diffraction patterns (XRD) of the samples were measured by using a Bruker Scintag powder diffractometer. GC-MS was measured with a HP 5971 GC-MS spectrometer. The solution  $^1\text{H}$  NMR spectrum was measured by using a Bruker DPX-300 NMR spectrometer. The FTIR spectrum was measured on a Nicolet IR 200 by dissolving the 4-(4-nitrophenyl)morpholine in ethanol and casting a drop of the solution on a KBr disc. A drop of the solution was kept on a KBr disc and air-dried before measuring. X-ray photoelectron spectra (XPS) were obtained by using a Surface Science Instrument SSX-100. The dynamic light scattering experiments were performed with a Brookhaven 90Plus Dynamic Light Scattering setup with a BI-9000AT Digital autocorrelator.

**Catalysis:** In a typical C–N coupling reaction, a 50 mL three-necked round bottom flask was charged with *p*-nitrobenzyl chloride (1 mmol), morpholine (1.1 mmol), cesium carbonate (2 mmol), and Cu nanoparticles (0.025 mmol) in DMSO (5 mL). To prepare the Cu nanoparticles in DMSO, an aqueous solution of Cu nanoparticles (5 mL) prepared from a solution of PAA (1.33 mM) were centrifuged. After decanting the water and washing the nanoparticles with DMSO once, the particles were dispersed in DMSO (5 mL). The reaction mixture was heated to 120°C for 2.5 h. Upon completion, the reaction mixture was extracted by using dichloromethane and the organic extract was dried over anhydrous sodium sulfate to give the desired 4-(4-nitrophenyl)morpholine as a crystalline solid. The formation of the reaction product was confirmed by GC–MS,  $^1\text{H}$  NMR, and FTIR spectroscopy and its yield was determined to be 99% by GC.  $^1\text{H}$  NMR (300 MHz,  $\text{CDCl}_3$ ):  $\delta=8.12$  (d, 2H; aromatic  $\text{CH}-\text{C}-\text{NO}_2$ ), 7.52 (d, 2H; aromatic  $\text{CH}$ ), 3.86 (t, 4H;  $\text{N}-\text{CH}_2$ ), 3.35 ppm (t, 24H;  $\text{O}-\text{CH}_2$ ); FTIR (KBr):  $\tilde{\nu}=2967, 2901$  (aromatic C–H stretching),  $1205\text{ cm}^{-1}$  (C–N stretching mode); GC–MS:  $m/z$ : 208.

For the Mannich reaction, acetophenone (1 mmol), benzaldehyde (1 mmol), and aniline (1 mmol) were mixed in methanol (10 mL) in a 50 mL round bottom flask and stirred under a nitrogen atmosphere at room temperature. To this solution, Cu nanoparticle (10 mol%, 50 nm) and cesium carbonate (200 mg) were added. The reaction mixture was

stirred at room temperature. The reaction product was characterized by GC after 24 h and 48 h.

## Acknowledgements

We gratefully acknowledge the financial assistance by the US National Science Foundation (NSF), CAREER Grant No. CHE-0645348 and NSF DMR-0804846 for this work. We thank Dr. Jonathan Shu at Cornell University for his help with the XPS measurement. We also thank Prof. Qingrong Huang at Rutgers for allowing us to use the dynamic light scattering instrument in his lab and for some valuable discussion on the results.

- [1] Y. Xia, Y. Xiong, B. Lim, S. E. Skrabalak, *Angew. Chem.* **2009**, *121*, 62–108; *Angew. Chem. Int. Ed.* **2009**, *48*, 60–103.
- [2] a) A. R. Tao, S. Habas, P. Yang, *Small* **2008**, *4*, 310–325; b) P. Pergolese, M. Muniz-Miranda, A. Bigotto, *J. Phys. Chem. A* **2006**, *110*, 9241–9245.
- [3] M. C. Daniel, D. Astruc, *Chem. Rev.* **2004**, *104*, 293–346.
- [4] N. L. Rosi, C. A. Mirkin, *Chem. Rev.* **2005**, *105*, 1547–1562.
- [5] a) C. F. Monson, A. T. Woolley, *Nano Lett.* **2003**, *3*, 359–363; b) J. A. Eastman, S. U. S. Choi, S. Li, W. Yu, L. J. Thompson, *Appl. Phys. Lett.* **2001**, *78*, 718–720.
- [6] L. Lu, M. Sui, K. Lu, *Science* **2000**, *287*, 1463–1466.
- [7] a) J. J. Brege, C. E. Hamilton, C. A. Crouse, A. R. Barron, *Nano Lett.* **2009**, *9*, 2239–2242; b) T. Ghodselahi, M. A. Vesaghi, A. Shafiekhani, A. Baghizadeh, M. Lameii, *Appl. Surf. Sci.* **2008**, *255*, 2730–2734; c) C. K. Wu, M. Yin, S. O'Brien, J. T. Koberstein, *Chem. Mater.* **2006**, *18*, 6054–6058; d) T. Y. Dong, H. H. Wu, C. Huang, J. M. Song, I. G. Chen, T. H. Kao, *Appl. Surf. Sci.* **2009**, *255*, 3891–3896; e) A. Galtayries, J.-P. Bonnelle, *Surf. Interface Anal.* **1995**, *23*, 171–179; f) S. K. Chawla, N. Sankarraman, J. H. Payer, *J. Electron Spectrosc. Relat. Phenom.* **1992**, *61*, 1–18; g) N. S. McIntyre, S. Sunder, D. W. Shoesmith, F. W. Stanchell, *J. Vac. Sci. Technol.* **1981**, *18*, 714–721; h) P. E. J. Larson, *J. Electron Spectrosc. Relat. Phenom.* **1974**, *4*, 213–218; i) P. E. Laibinis, G. M. Whitesides, *J. Am. Chem. Soc.* **1992**, *114*, 9022–9028; j) N. S. McIntyre, M. G. Cook, *Anal. Chem.* **1975**, *47*, 2208–2213; k) G. Deroubaix, P. Marcus, *Surf. Interface Anal.* **1992**, *18*, 39; l) C. D. Wagner, L. H. Gale, R. H. Raymond, *Anal. Chem.* **1979**, *51*, 466–482; m) T.-Y. Chen, S.-F. Chen, H.-S. Sheu, C.-S. Yeh, *J. Phys. Chem. B* **2002**, *106*, 9717–9722; n) H. Ron, H. Cohen, S. Matlis, M. Rappaport, I. Rubinstein, *J. Phys. Chem. B* **1998**, *102*, 9861–9869.
- [8] T. B. Ressler, L. Kniep, I. Kasatkin, R. Schlögl, *Angew. Chem.* **2005**, *117*, 4782–4785; *Angew. Chem. Int. Ed.* **2005**, *44*, 4704–4707.
- [9] S. Vukojevic, O. Trapp, J. Grunwaldt, C. Kiener, F. Schth, *Angew. Chem.* **2005**, *117*, 8192–8195; *Angew. Chem. Int. Ed.* **2005**, *44*, 7978–7981.
- [10] S. Park, R. J. Gorte, J. M. Vohs, *Appl. Catal. A* **2000**, *200*, 55–61.
- [11] M. P. Pileni, *Nat. Mater.* **2003**, *2*, 145–150.
- [12] I. Lisiecki, M. P. Pileni, *J. Am. Chem. Soc.* **1993**, *115*, 3887–3896.
- [13] C. Salzemann, J. Urban, I. Lisiecki, M. P. Pileni, *Adv. Funct. Mater.* **2005**, *15*, 1277–1284.
- [14] P. Cason, C. B. Roberts, *J. Phys. Chem. B* **2000**, *104*, 1217–1221.
- [15] I. Lisiecki, M. P. Pileni, *J. Phys. Chem.* **1995**, *99*, 5077–5082.
- [16] S. Wu, D. Chen, *J. Colloid Interface Sci.* **2004**, *273*, 165–169.
- [17] G. Zhou, M. Lu, Z. Yang, *Langmuir* **2006**, *22*, 5900–5903.
- [18] Y. Chang, M. L. Lye, H. C. Zeng, *Langmuir* **2005**, *21*, 3746–3748.
- [19] H. Huang, F. Yan, Y. Kek, C. Chew, G. Xu, W. Ji, P. Oh, S. Tang, *Langmuir* **1997**, *13*, 172–175.
- [20] M. J. Galkowski, L. Wang, J. Luo, C. Zhong, *Langmuir* **2007**, *23*, 5740–5745.
- [21] I. Pastoriza-Santos, A. Sánchez-Iglesias, B. Rodríguez-González, L. M. Liz-Marzán, *Small* **2009**, *5*, 440–443.
- [22] S. I. Cha, C. B. Mo, K. T. Kim, Y. J. Jeong, S. H. Hong, *J. Mater. Res.* **2006**, *21*, 2371–2378.

- [23] A. Banerjee, L. Yu, H. Matsui, *Proc. Natl. Acad. Sci. USA* **2003**, *100*, 14678–14682.
- [24] J. Wang, H. Huang, S. V. Kesapragada, D. Gall, *Nano Lett.* **2005**, *5*, 2505–2508.
- [25] G. Vitulli, M. Bernini, S. Bertozzi, E. Pitzalis, P. Salvadori, S. Coluccia, G. Martra, *Chem. Mater.* **2002**, *14*, 1183–1186.
- [26] a) J. Wang, T. Yang, W. Wu, L. Chen, C. Chen, C. Chu, *Nanotechnology* **2006**, *17*, 719–722; b) C. Kim, W. Gu, M. Briceno, I. M. Robertson, H. Choi, K. Kim, *Adv. Mater.* **2008**, *20*, 1859–1863; c) H. Choi, S. H. Park, *J. Am. Chem. Soc.* **2004**, *126*, 6248–6249.
- [27] A. Henglein, *J. Phys. Chem. B* **2000**, *104*, 1206–1211.
- [28] S. Kapoor, D. K. Palit, T. Mukherjee, *Chem. Phys. Lett.* **2002**, *355*, 383–387.
- [29] R. Vijaya Kumar, Y. Mastai, Y. Diamanta, A. Gedanken, *J. Mater. Chem.* **2001**, *11*, 1209–1213.
- [30] W. Wang, G. Wang, X. Wang, Y. Zhan, Y. Liu, C. Zheng, *Adv. Mater.* **2002**, *14*, 67–69.
- [31] J. Hambrook, R. Becker, A. Birkner, J. Weiß, R. A. Fischer, *Chem. Commun.* **2002**, 68–69.
- [32] A. Yanase, H. Komiyama, *Surf. Sci.* **1991**, *248*, 11–19.
- [33] J. Ziegler, R. C. Doty, K. P. Johnston, B. A. Korgel, *J. Am. Chem. Soc.* **2001**, *123*, 7797–7803.
- [34] C. Salzemann, A. Brioude, M. P. Pileni, *J. Phys. Chem. B* **2006**, *110*, 7208–7212.
- [35] C. Salzemann, I. Lisiecki, A. Brioude, J. Urban, M. P. Pileni, *J. Phys. Chem. B* **2004**, *108*, 13242–13248.
- [36] H. Huang, X. Ni, G. L. Loy, C. H. Chew, K. Tan, F. C. Loh, J. Deng, G. Xu, *Langmuir* **1996**, *12*, 909–912.
- [37] S. M. Heard, F. Grieser, C. G. Barraclough, J. V. Sanders, *J. Colloid Interface Sci.* **1983**, *93*, 545–555.
- [38] S. Panigrahi, S. Kundu, S. K. Ghosh, S. Nath, S. Praharaj, S. Basu, T. Pal, *Polyhedron* **2006**, *25*, 1263–1269.
- [39] P. Y. S. Lam, S. Deudon, K. M. Averill, R. H. Li, M. Y. He, P. De-Shong, C. G. Clark, *J. Am. Chem. Soc.* **2000**, *122*, 7600–7601.
- [40] C. Almansa, J. Bartrolí, J. Belloc, F. L. Cavalcanti, R. Ferrando, L. A. Gómez, I. Ramis, E. Carceller, M. Merlos, J. García-Rafanell, *J. Med. Chem.* **2004**, *47*, 5579–5582.
- [41] T. Güngör, A. Fouquet, J. M. Teulon, D. Provost, M. Cazes, A. Cloarec, *J. Med. Chem.* **1992**, *35*, 4455–4463.
- [42] W. A. Herrmann, *Angew. Chem.* **2002**, *114*, 1342–1363; *Angew. Chem. Int. Ed.* **2002**, *41*, 1290–1309.
- [43] a) W. Anderson, R. E. Tundel, T. Ikawa, R. A. Altman, S. L. Buchwald, *Angew. Chem.* **2006**, *118*, 6673–6677; *Angew. Chem. Int. Ed.* **2006**, *45*, 6523–6527; b) G. Mann, J. F. Hartwig, M. S. Driver, C. Fernandez-Rivas, *J. Am. Chem. Soc.* **1998**, *120*, 827–828; c) S. Uk Son, I. K. Park, J. Park, T. Hyeon, *Chem. Commun.* **2004**, 778–779; d) G. G. Jernigan, G. A. Somorjai, *J. Catal.* **1994**, *147*, 567–577; e) T. J. Huang, D. H. Tsai, *Catal. Lett.* **2003**, *87*, 173–178; f) P. O. Larsson, A. Andersson, *J. Catal.* **1998**, *179*, 72–89.
- [44] R. Narayanan, M. A. El-Sayed, *J. Phys. Chem. B* **2005**, *109*, 12663–12676.
- [45] A. Zecchina, E. Groppo, S. Bordiga, *Chem. Eur. J.* **2007**, *13*, 2440–2460.
- [46] M. L. Kantam, J. Yadav, S. Laha, B. Sreedhar, S. Jha, *Adv. Synth. Catal.* **2007**, *349*, 1938–1942.
- [47] a) B. White, M. Yin, A. Hall, D. Le, S. Stolbov, T. Rahman, N. Turro, S. O'Brien, *Nano Lett.* **2006**, *6*, 2095–2098; b) M. Samim, N. K. Kaushik, A. Maitra, *Bull. Mater. Sci.* **2007**, *30*, 535–540.

Received: February 10, 2010  
Published online: July 20, 2010